Engineering

Industrial & Management Engineering fields

Okayama University *Year* 2004

On-line actuator state monitoring of a MIMO bioprocess

Mingcong Deng
Okayama University

Akira Inoue
Okayama University

Kazushi Ishikawa
Okayama University

Yoichi Hirashima
Okayama University

On-line actuator state monitoring of a MIMO bioprocess

Mingcong Deng
Okayama University,

Akira Inoue
Okayama University,

Kazushi Ishikawa
Okayama University,

Yoichi Hirashima
Okayama University,

On-line actuator state monitoring of a MIMO bioprocess

Mingcong Deng
Okayama University,

Akira Inoue
Okayama University,

Kazushi Ishikawa
Okayama University,

Yoichi Hirashima
Okayama University,

2004 5th Asian Control Conference

On-line Actuator State Monitoring of a MIMO Bioprocess

Mingcong Deng, Akira Inoue, Kazushi Ishikawa, and Yoichi Hirashima
Department of Systems Engineering, Okayama University
3-1-1 Tsushima-naka, Okayama 700-8530, Japan
deng@suri.sys.okayama-u.ac.jp

Abstract

In the actuator state monitoring of a time varying human multijoint arm dynamics, typical issues are compounded by problems related to the uncertainty factor consisting of measurement noises and modeling error of the rigid body dynamics. In general, the uncertainty factor is under the case of non-Gaussian noises. In this paper, for improving the monitoring, a robust filter system based on a score function approach is modified. The score function is associated with $\bar{U}D$ factorization algorithm. The selection of the shape parameter in the monitoring filter is discussed. Examples of the proposed method for an experiment-based human arm model show better accuracy and robustness compared with standard Kalman filter.

1 Introduction

Much attention has been paid to the problem of fault detection and diagnosis in many industrial processes and bioprocesses. One of the most interesting approaches is of detecting and diagnosing actuator states. The actuator states are considered as arm viscoelasticity. Especially, life system actuator parameters are adjusted directly based on physical change and motor command from central nervous system (CNS). For example, human arm is derived by the multijoint muscle generated torque, which is assumed to be a function of angular position, velocity and motor command of CNS. The change of the torque is caused by arm viscoelasticity. And the arm viscoelasticity consists of joint stiffness, which is regulated by muscle inherent spring-like properties and neural feedbacks, and viscosity. Therefore, to estimate joint stiffness and viscosity properties of arm is important in regulating posture and movement, and interacting environments.

For the estimation of the actuator state during voluntary movements, alternative method using single trial data was reported for multijoint joint movements [5] based on Kalman filter. However, the estimate can be degraded under the existence of arm modeling error and measurement noises, because the above uncertainty factor is highly non-Gaussian. In the non-Gaussian environment, one of the most effective schemes ever proposed [1] is based on the nonlinear score function approach [7, 8] by extending the design scheme given in [2]. Compared with standard Kalman filter, for human arm innovations process including the measurements of multijoint muscle generated torque, the design scheme achieves significant improvements with respect to stationary mean square error and rate of convergence. The ill-conditioned covariance update equation of the estimator and a derivative of the score function in the covariance update equation are avoided. Because the method does not require many trials, the effect of subject for each trial can be extremely reduced and physical change from trial to trial can be avoided. In this paper, the above recursive filter design method is modified. For improvement of the on-line estimation characteristics, the selection of the shape parameter in the monitoring filter is discussed.

2 Human Arm Dynamics Model

In this paper, the arm viscoelasticity is defined as actuator state. Therefore, the problem is to estimate the viscoelasticity from measured data of the multijoint muscle generated torques. To estimate the viscoelasticity, the human arm dynamics and pseudo-random perturbation method are introduced. Two-link rigid human arm dynamics on the horizontal plane can be modeled by the following equation [4].

$$\begin{pmatrix} Z_1 + 2Z_2 cos\theta_2 & Z_3 + Z_2 cos\theta_2 \\ Z_3 + Z_2 cos\theta_2 & Z_3 \end{pmatrix}(q)\ddot{q} + \begin{pmatrix} -Z_2 sin\theta_2(\dot{\theta_2}^2 + 2\dot{\theta}_1\dot{\theta}_2) \\ Z_2\dot{\theta_1}^2 sin\theta_2 \end{pmatrix}(\dot{q}, q) = \tau_{in}(\dot{q}, q, u) + \tau_{ext} \quad (1)$$

where, $\tau_{ext} = [\tau_{s\_ext}, \tau_{e\_ext}]^T$ denotes the external force, the subscripts s and e denote shoulder and elbow, respectively. τ_{in} is the multijoint muscle generated torque, which is assumed to be a function of angular position, velocity and motor command u. q, $\dot{q}$ and $\ddot{q}$ are angular position, velocity and acceleeration vector, respectively,where

$$q = (\theta_1(t), \theta_2(t))^T$$
$$\tau_{in} = (\tau_s, \tau_e)^T \quad (2)$$

$\theta_1(t)$ is shoulder angle and $\theta_2(t)$ is elbow angle shown in Fig.1. Z_1, Z_2 and Z_3 are structural dependent parameters. For estimating arm viscoelasticity, a pseudo-random perturbation that contains sufficient frequency components is employed. Because multijoint muscle generated torque, τ_{in}, is a function of position, velocity, and motor command, its variational component, $\delta\tau_{in}$, can be represented as follows.

$$\delta\tau_{in} = -\boldsymbol{D}\delta\dot{\boldsymbol{q}} - \boldsymbol{R}\delta\boldsymbol{q} + \frac{\partial\tau_{in}}{\partial u}\delta u \tag{3}$$

Here, $\boldsymbol{D}$ and $\boldsymbol{R}$ present muscle viscosity and stiffness matrix, and

$$\begin{aligned} -\frac{\partial\tau_{in}}{\partial\dot{\boldsymbol{q}}^T} &= \boldsymbol{D} = \begin{pmatrix} D_{ss} & D_{se} \\ D_{es} & D_{ee} \end{pmatrix} \\ -\frac{\partial\tau_{in}}{\partial\boldsymbol{q}^T} &= \boldsymbol{R} = \begin{pmatrix} R_{ss} & R_{se} \\ R_{es} & R_{ee} \end{pmatrix} \end{aligned} \tag{4}$$

The subscripts ss of D and R represent the shoulder single-joint effect on each coefficient. Similarly, se and es denote cross-joint effects, and ee denotes the elbow single-joint effect. Here, the term of $\frac{\partial\tau_{in}}{\partial u}\delta u$ can be neglected by applying band-pass filtering [5]. The problem considered in this paper is to estimate D and R from measured data of multijoint muscle generated torques.

3 Design of Actuator State Monitoring Filter

By using a band-pass filter for the model (1), the filtered torque τ_{in}^f, the filtered positions $\theta_1^f(t)$ and $\theta_2^f(t)$, and the filtered velocities $\dot{\theta}_1^f(t)$ and $\dot{\theta}_2^f(t)$ satisfy the relation: $\tau_{in}^f = XU + \Delta + \zeta_1$, where X is the regression vector, U is the time-varying parameter vector to be estimated, and where

$$\begin{aligned} X &= \begin{pmatrix} \theta_1^f & \theta_2^f & \dot\theta_1^f & \dot\theta_2^f & 0 & 0 & 0 & 0 \\ 0 & 0 & 0 & 0 & \theta_1^f & \theta_2^f & \dot\theta_1^f & \dot\theta_2^f \end{pmatrix} \\ U &= \begin{pmatrix} R_{ss} & R_{se} & D_{ss} & D_{se} & R_{es} & R_{ee} & D_{es} & D_{ee} \end{pmatrix}^T \end{aligned} \tag{5}$$

where $\Delta = [\Delta_1, \Delta_2]^T$ consists of the structured uncertainty of the left side of (1). The uncertainty is from human arm parameter (i.e., Z_i). Following the score function, Δ_1 and Δ_2 are assumed to be Gaussian, $\zeta_1 = [\bar{\zeta}_{11}, \bar{\zeta}_{22}]^T$ is the non-Ganssian measurement error matrix of τ_{ext}. In the actual estimation, the above uncertainty factor should be considered to avoid estimation errors. In this paper, to reduce the effect of the uncertainty factor, we will consider a filtering algorithm for estimating multijoint human arm viscoelasticity.

To design the filtering algorithm, we need to prepare the above model in the discrete time state-space form as follows.

$$\begin{aligned} &U(t+1) = U(t) + \zeta_2, \quad t = 1, 2, \cdots \\ &\tau_{in}^f(t+1) = X(t+1)U(t) + \Delta(t) + \zeta_1(t) \end{aligned} \tag{6}$$

where, ζ_2 is white noise, $\Delta(t) = C(z^{-1})\zeta_2$, $\zeta_2 = [\zeta_{21}, \cdots, \zeta_{28}]^T$ and

$$\begin{aligned} C(z^{-1}) &= \begin{pmatrix} C_1(z^{-1}) \\ C_2(z^{-1}) \end{pmatrix} = \begin{pmatrix} \sum_{i=0}^{n_c} C_{1,i} z^{-1} \\ \sum_{i=0}^{n_c} C_{2,i} z^{-1} \end{pmatrix} \\ C_{j,i} &= [C_{j,i1}, \cdots, C_{j,i8}], \quad j = 1, 2 \end{aligned} \tag{7}$$

The fundamental problem associated with human arm system is to estimate viscoelasticity by using the generated torques τ_s and τ_e. Here, we consider a matrix disturbance sequence instead of multi-dimensional $C(z^{-1})\zeta_2$. Then, the design method can be extended to multiple innovations process [1]. We can calculate variance $\sigma_{\Delta_i}^2 (i = 1, 2)$ of element of the new matrix disturbance sequence, where, $\bar{\zeta}_2 = \sum_{i=1}^{8} \zeta_{2i}$. In the following, the problem is to design the recursive filter based on score function approach [7] for the arm model with uncertainty factor. The score function approach along with generalized Gaussian approximation of the innovations process probability density function (pdf) can be used for state estimation of non-Gaussian system. The shape parameter of the pdf controls the shape of the distribution. The pdf of generalized Gaussian uncertainty factor $\Delta_i(t) + \bar{\zeta}_{ii}(t) (i = 1, 2)$ with zero mean, variance σ_i^2 and shape parameter γ_i is given by [6]

$$\begin{aligned} p_i(x_i; \sigma_i, \gamma_i) &= \frac{\alpha_i(\gamma_i)\gamma_i}{2\sigma_i\Gamma(1/\gamma_i)} e^{-[\alpha_i(\gamma_i)|x_i/\sigma_i|]^{\gamma_i}} \\ x_i &\in R, \quad i = 1, 2 \end{aligned} \tag{8}$$

$$\alpha_i(\gamma_i) = \sqrt{\frac{\Gamma(3/\gamma_i)}{\Gamma(1/\gamma_i)}} \tag{9}$$

where $\Gamma(\cdot)$ is the Gamma function. If $\gamma_i = 2$, the uncertainty factor is completely characterized by its second-order moment. Otherwise, the uncertainty factor is completely characterized by its second-order moment and fourth-order moment. In the paper of [1], the shape parameter is determined by the one-to-one correspondence between γ_i and the following fourth-order even moment

$$\phi_i(\gamma_i) = \frac{E(\tau_i^4)}{\sigma_i^4} = \frac{\Gamma(5/\gamma_i)\Gamma(1/\gamma_i)}{\Gamma^2(3/\gamma_i)} \tag{10}$$

where

$$\begin{aligned} E(\tau_i^4) &= \phi_i(\gamma_i)\sigma_i^4 \\ &= \sigma_{\Delta_i}^4 \phi_i(\gamma_{\Delta_i}) + \sigma_{\bar\zeta_{ii}}^4 \phi_i(\gamma_{\bar\zeta_{ii}}) + 6\sigma_{\Delta_i}^2 \sigma_{\bar\zeta_{ii}}^2 \quad (11) \\ \sigma_i^2 &= \sigma_{\Delta_i}^2 + \sigma_{\bar\zeta_{ii}}^2 \quad (12) \\ \phi_i(\gamma_{\Delta_i}) &= \phi_i(2) = 3 \quad (13) \end{aligned}$$

where $\sigma_{\Delta_i}^2$, γ_{Δ_i}, $\sigma_{\bar\zeta_{ii}}^2$ and $\gamma_{\bar\zeta_{ii}}$ are variance of Δ_i, shape parameter of Δ_i, variance of $\bar\zeta_{ii}$ and shape parameter of $\bar\zeta_{ii}$, respectively. The odd moments vanish, because the pdf is the symmetry.

In this paper, we consider an approximated relation from (10) as

$$\phi_i(\gamma_i) = \frac{l_{2i}e^{-l_{1i}\gamma_i}}{\sigma_i^4} \tag{14}$$

where the design parameters l_{0i} and l_{1i} can be obtained by matching (10) in pre-experiment. The unmatched part will be of uncertainty factor. Using the result in [2], the proposed algorithm guarantees that all the estimated elements of viscoelasticity are bounded (The proof is omitted).

Considering the generalized Gaussian pdf given in (10), the score function-based algorithm [1, 2] is obtained.

$$\hat{U}(t+1) = \hat{U}(t) + k(t)\begin{pmatrix} \gamma_1(\frac{\alpha_1(\gamma_1)}{\sigma_1})^{\gamma_1}\tau_1^{\gamma_1-1} \\ \gamma_2(\frac{\alpha_2(\gamma_2)}{\sigma_2})^{\gamma_2}\tau_2^{\gamma_2-1} \end{pmatrix} \tag{15}$$

$$\tau_i > 0 (i = 1, 2), \tau_1 = \tau_s, \tau_2 = \tau_e$$

$$k(t) = (W(t)N(t)W(t)^T + L)X^T \tag{16}$$

where $N(t)$ is a diagonal matrix and $W(t)$ is an upper-triangular matrix with unit entries along the diagonal [1]. L is positive definite and is the covariance matrix of ζ_2. $\hat{U}$ is an estimate parameter vector of U.

4 Simulation Model and Results

The structural parameters Z_1, Z_2 and Z_3 are unknown, and in the simulation we select the true values of the parameters as $Z_1 = 0.4507$, $Z_2 = 0.1575$ and $Z_3 = 0.1530$ based on the result in [3, 4]. The error range is selected as 0.05%. The cut-off frequencies of the third-order band-pass filter to generate τ_{in}^f, $\theta_i^f(t)$ and $\dot{\theta}_i^f(t)$ are 2.5[Hz] and 20[Hz]. Besides the above 0.05% uncertainty the filtered noise applied in τ_{in}^f is

$$\begin{pmatrix} 0.09 + 0.045 * rand(r_1) \\ 0.09 + 0.045 * rand(r_2) \end{pmatrix}$$

where, $rand(r_i)$ is a function to generate random noise with the initial value r_i.

During multijoint viscoelasticity measurement, the arm model was instructed to move from the start position (x,y)=[-0.2,0.35](m) to the end position (x,y)=[0.2,0.35](m) directly (Fig. 1 [1, 2]). The arm simulation procedure is described as follows. The arm keeps unmoving at the start position for $1s$, then it moves in the uniform velocity for $3s$ and keeps unmoving at end position for $1s$. The whole simulation time is $5s$. External torque produced by random are the filtered torque of $\tau_{s\_ext} = 40 * (rand(r_3) - 0.5)$ and $\tau_{e\_ext} = 30 * (rand(r_4) - 0.5)$ by fourth order Butterworth filter. For shoulder, the filter cut-off frequency is 4Hz $\sim$ 16Hz. For elbow, the filter cut-off frequency is 8Hz $\sim$ 24Hz, where $rand(r_3)$ and $rand(r_4)$ are random signals. Using the conventional Kalman filter to estimate viscoelastic parameters for the model with uncertainty, Fig.2 shows the mean error of the estimation of the arm model with 5% uncertainty of Z_i [1, 2].

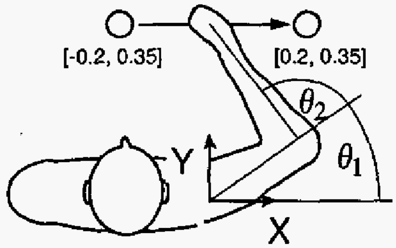

Figure 1: One of the movement descriptions of the arm model

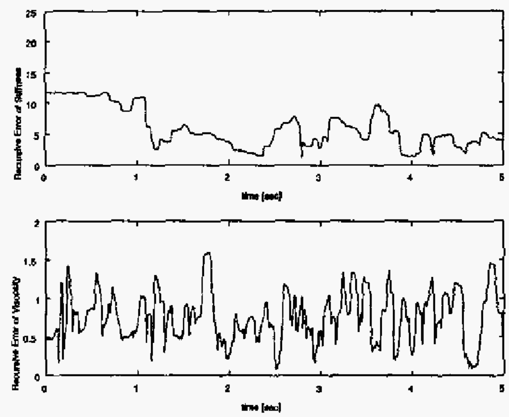

Figure 2: Time-variation of mean error of stiffness and viscosity by using Kalman filter with 5% uncertainty of Z_i

Considering the estimation algorithm given in Section 3, the simulation results are shown in Figs. 3 and 4, where $l_{21} = l_{22} = 8.974$, $l_{11} = l_{12} = 1.034e^9$. In these simulations, the design parameters are the same, but the $\bar{U}D\bar{U}^T$ term is added, further, uncertainty and noise treatment are also considered. Comparing the simulation results, the proposed algorithm shows a better performance. Fig. 4 shows the stiffness ellipses calculated from these data during movement. The ellipses represent the direction and magnitude of elastic, resisting forces to unit-length position perturbations in all directions. The long axis of each ellipse represents maximum force, indicating the greatest stiffness. The short axis represents minimum force, indicating the least stiffness [3, 4].

In the following, to show the effect of difference of movements, three simulations with different movements are conducted (see Table 1).

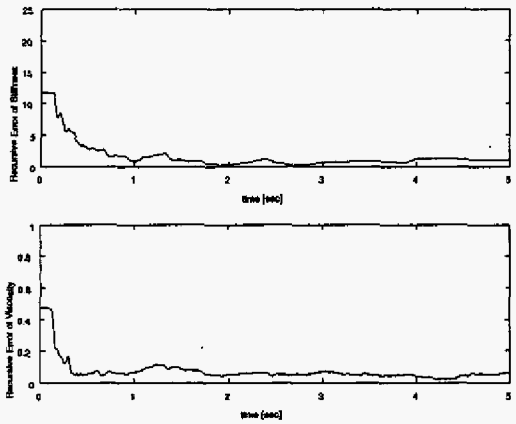

Figure 3: Time-variation of mean error of stiffness and viscosity by using the proposed algorithm with 5% uncertainty of Z_i

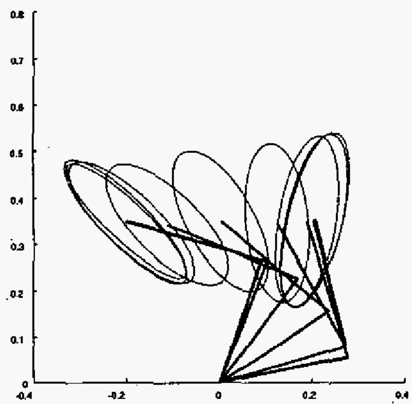

Figure 4: Stiffness ellipse estimated by using the proposed algorithm with 5% uncertainty of Z_i

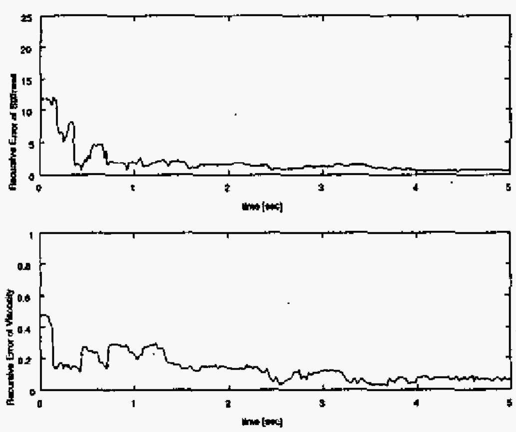

Figure 5: Time-variation of mean error of stiffness and viscosity by using the algorithm in [1] with 5% uncertainty of Z_i

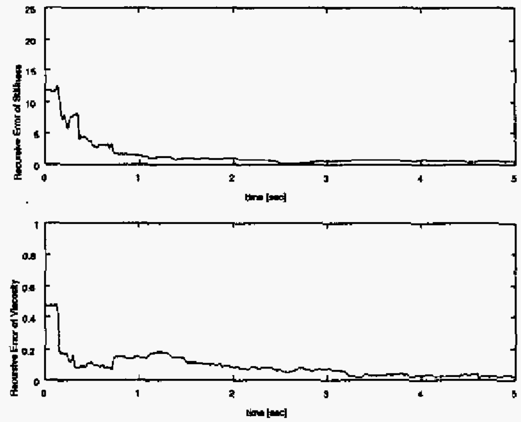

Figure 6: Time-variation of mean error of stiffness and viscosity by using the proposed algorithm with 5% uncertainty of Z_i

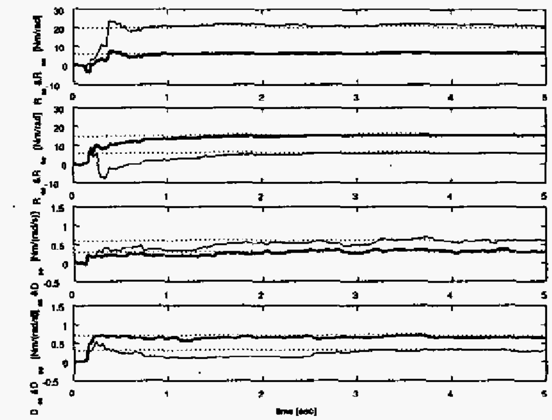

Figure 7: Estimated stiffness and viscosity by using the proposed algorithm with 5% uncertainty of Z_i

Simulation run	Movements
1(5% err)	[-0.2,0.35] to [0.2,0.35]
2(5% err)	[0,0.5] to [0,0.2]
3(5% err)	[-0.2,0.4465] to [0.2,0.4465]
4(5% err)	[-0.2,0.25] to [0.2,0.45]

Table 1

During multijoint viscoelasticity measurement, under the same design condition with the proposed robust filter in the case of 5% uncertainty of Z_i, the arm model was instructed to move from the start position (x,y)=[0,0.5](m) to the end position (x,y)=[0,0.2](m) directly. Mean error of the estimation, the estimated viscoelasticity and stiffness ellipse of the arm model are described in Figs. 6 $\sim$ 8. Considering the estimation algorithm given in [1], as the same uncertainty with the above simulation, the simulation result is shown in Fig.5. Comparing the simulation results, the proposed algorithm shows a better performance.

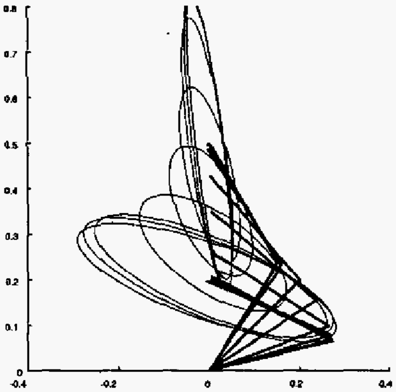

Figure 8: Stiffness ellipse estimated by using the proposed algorithm with 5% uncertainty of Z_i

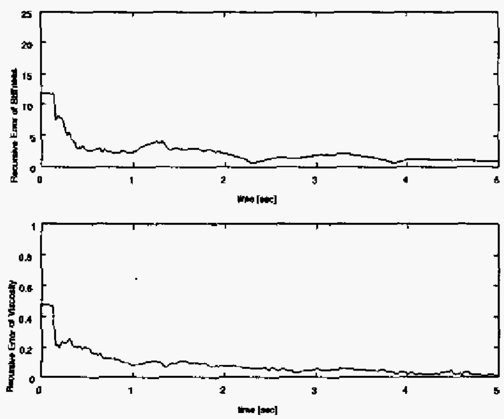

Figure 9: Time-variation of mean error of stiffness and viscosity by using the proposed algorithm with 5% uncertainty of Z_i

Meanwhile, for the case of the arm model being instructed to move from the start position (x,y)=[-0.2,0.4465](m) to the end position (x,y)=[0.2,0.4465](m) as an arc, the simulation results are shown in Figs. 9 and 10. For the case of the arm model being instructed to move from the start position (x,y)=[-0.2,0.25](m) to the end position (x,y)=[0.2,0.45](m) directly, the simulation results are shown in Figs. 11 and 12. Based on the above simulation results, the influence from the moving directions is not so large. In this paper, all of the dotted lines in Fig. 7 describe the corresponding true values based on the following relationships [3, 4].

$$R_{ss} = A_{ss}|\tau_{s\_m}| + B_{ss} \quad (17)$$

$$R_{se} = A_{se}|\tau_{e\_m}| + B_{se} \quad (18)$$

$$R_{es} = R_{se} \quad (19)$$

$$R_{ee} = A_{ee}|\tau_{e\_m}| + B_{ee} \quad (20)$$

$$D_{ss} = C_{ss}|\tau_{s\_m}| + E_{ss} \quad (21)$$

$$D_{se} = C_{se}|\tau_{e\_m}| + E_{se} \quad (22)$$

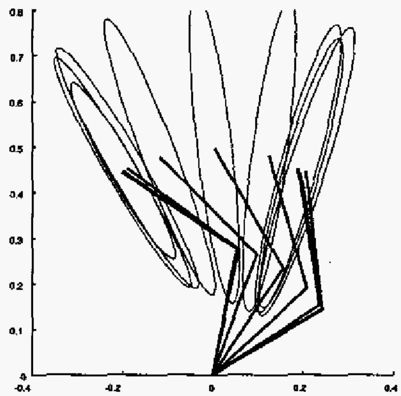

Figure 10: Stiffness ellipse estimated by using the proposed algorithm with 5% uncertainty of Z_i

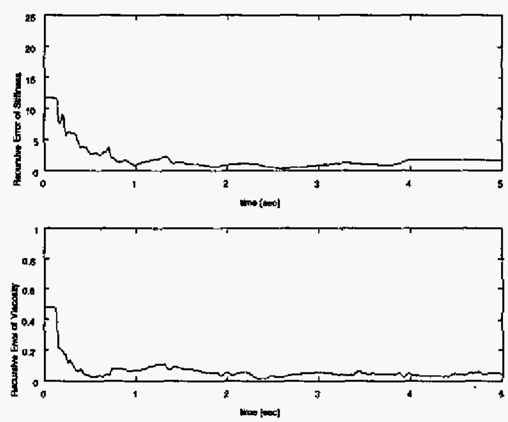

Figure 11: Time-variation of mean error of stiffness and viscosity by using the proposed algorithm with 5% uncertainty of Z_i

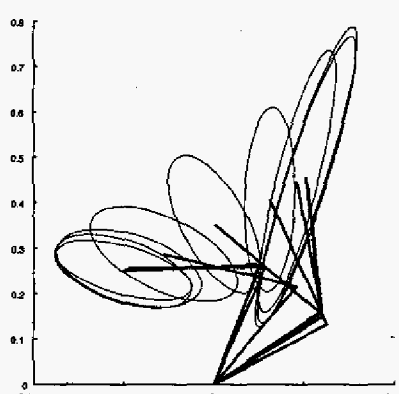

Figure 12: Stiffness ellipse estimated by using the proposed algorithm with 5% uncertainty of Z_i

$$D_{es} = D_{se} \quad (23)$$
$$D_{ee} = C_{ee}|\tau_{e\_m}| + E_{ee} \quad (24)$$

where

$$\begin{pmatrix} \tau_{s\_m} \\ \tau_{e\_m} \end{pmatrix} = \boldsymbol{I}(\boldsymbol{q}_d)\ddot{\boldsymbol{q}}_d + \boldsymbol{H}(\dot{\boldsymbol{q}}_d, \boldsymbol{q}_d) \quad (25)$$

τ_{s_m} and τ_{e_m} are the desired shoulder and elbow torques, respectively. $\boldsymbol{q}_d$ is the desired angular position vector. And

$$\begin{aligned} A_{ss} &= 20, \ B_{ss} = 20 \\ A_{se} &= 12, \ B_{se} = 6 \\ A_{ee} &= 28, \ B_{ee} = 15 \\ C_{ss} &= 0.6, \ E_{ss} = 0.6 \\ C_{se} &= 0.4, \ E_{se} = 0.3 \\ C_{ee} &= 0.8, \ E_{ee} = 0.7 \quad (26) \end{aligned}$$

where, the estimation results are evaluated by using the following formulations.

$$E_R = (|\Delta R_{ss}| + |\Delta R_{se}| + |\Delta R_{es}| + |\Delta R_{ee}|)/4$$
$$E_D = (|\Delta D_{ss}| + |\Delta D_{se}| + |\Delta D_{es}| + |\Delta D_{ee}|)/4$$

In the simulation, the multijoint muscle generated torque is obtained as follows.

$$\tau_{in} = R(\boldsymbol{q}_{eq} - \boldsymbol{q}) - D\dot{\boldsymbol{q}} \quad (27)$$

where $\boldsymbol{q}_{eq}$ is the equilibrium point. Note that $E(\tau_i^4) = l_{2i}e^{-l_{1i}\gamma_i}$ from (10) and (14). $E(\tau_i^4)$ is solved for each processing time step, then the shape parameter is given as follows.

$$\gamma_i = -\frac{1}{l_{1i}} log(E/l_{2i}) \quad (28)$$
$$E(\tau_i^4) = \sigma_{\Delta_i}^4 \phi_i(\gamma_{\Delta_i}) + \sigma_{\zeta_{ii}}^4 \phi_i(\gamma_{\zeta_{ii}}) + 6\sigma_{\Delta_i}^2 \sigma_{\zeta_{ii}}^2 \quad (29)$$
$$\sigma_{\Delta_1}^2 = XMX^T(1,1) \quad (30)$$
$$\sigma_{\Delta_2}^2 = XMX^T(2,2) \quad (31)$$

5 Conclusion

In order to improve the actuator state monitoring of a human multijoint arm dynamics, a robust filter system is modified. The selection of the shape parameter is discussed. Compared with standard Kalman filter, examples of the proposed method obtaining desired accuracy and robustness are given.

References

[1] M. Deng, A. Inoue, H. Gomi, and Y. Hirashima, *Recursive filter design for estimating time varying multijoint human arm viscoelasticity*, Int. J. of Comp., Sys. and Signals, Vol.4, No. 2, 2003.

[2] M. Deng and H. Gomi, *Robust estimation of human multijoint arm viscoelasticity during movement*, Trans. of the Soc. of Instrument and Control Engineers, Vol. 39, pp. 537-543, 2003(in Japanese).

[3] H. Gomi and M. Kawato, *Equilibrium-point control hypothesis examined by measured arm-stiffness during multi-joint movement*, Science, Vol. 272, pp. 117-120, 1996.

[4] H. Gomi and M. Kawato, *Human arm stiffness and equilibrium-point trajectory during multi-joint movement*, Biological Cybernetics, Vol. 76, pp. 163-171, 1997.

[5] H. Gomi and T. Konno, *Real time estimation of time-varying human multijoint arm viscoelasticity during movements*, Proc. of 20th Annual Int. Con. of the IEEE Eng. in Med. and Bio. Soci., Vol.20, No.5, pp.2341-2342, 1998.

[6] W. Niehsen, *Generalized Gaussian modeling of correlated signal sources*, IEEE Trans. Signal Processing, Vol. 47, pp. 217-219, 1999.

[7] W. Niehsen, *Robust Kalman filtering with generalized Gaussian measurement noise*, IEEE Trans. Aero. and Electr. Sys., Vol. 38, pp. 1409-1412, 2002.

[8] W. Wu and A. Kundu, *Recursive filtering with non-Gaussian noises*, IEEE Trans. Signal Processing, Vol. 44, pp. 1454-1468, 1996.